Characterization of Atmospheric Particulate Matter in Oil-Resource Cities and its Impact on Health: Daqing City, Northeast China

Lei Xu [1], Jiawen Shi [1], Chunsheng Fang [2,*]

1 Department of Environmental Science and Engineering, School of Chemistry and Environmental Engineering, Changchun University of Science and Technology, Changchun 130022, China
2 Department of Environmental Science, College of New Energy and Environment, Jilin University, Changchun 130012, China

Abstract. Atmospheric pollution can affect human production life and physical and mental health to a great extent. In this paper, the hourly pollutant monitoring data from five state-controlled automatic atmospheric monitoring stations in Daqing City from 2017 to 2021 are collected to analyze the temporal and spatial variation patterns of CO, SO_2, NO_2, $PM_{2.5}$, PM_{10}, O_3. And to assess the health risks of atmospheric particulate matter. The HYSPLIT model is applied to analyze air pollutants' transport pathways and the potential source areas of atmospheric particulate matter with the PSCF model. The results show that the concentrations of SO_2 and NO_2 are higher in the north of Daqing and the concentrations of pollutants generally show a decreasing trend with time. The hazard quotient (HQ) for atmospheric particulate matter, which is slightly above the safe range set by the EPA, is higher in winter and spring. After principal component analysis, CO, NO_2, and PM_{10} are the main factors affecting $PM_{2.5}$. In the summer, the main urban area's air pollution is mostly influenced by the southwest pollution trajectory. In other seasons, the northwest route predominantly regulates the regional transfer of contaminants. The key regions that could be the sources of atmospheric particulate matter include North China, Inner Mongolia, Mongolia, and Russia.

1. Introduction

In China, especially in northeast China, the problem of atmospheric pollution has become increasingly prominent, causing severe impacts on people's daily lives and physical and mental health, and has become a significant livelihood issue. [1,2]. Daqing is the only provincial ecological city in Heilongjiang Province, the most extensive petrochemical base in China. However, there are still severe air pollution phenomena. To promote the planning and prevention of air pollution and reduce regional air pollution, this study takes the jurisdiction of Daqing city as the study area and statistically analysis the pollution characteristics of six air pollutants (CO, SO_2, NO_2, O_3, $PM_{2.5}$, and PM_{10}) from 2017 to 2021, including the spatial and temporal variation characteristics of pollutants, spatial distribution characteristics, analysis of the health effects of atmospheric particulate matter and uses the potential source Contribution Function (PSCF) method was used to analysis and discuss the potential source areas of $PM_{2.5}$ and PM_{10}. The influence of regional transport on pollutant concentrations in Daqing City was also analysis, aiming to provide theoretical support for the prevention and control of atmospheric environmental pollution in Daqing City.

2. Methods

2.1. Research Areas and Data Sources

The mass concentrations of pollutants from January 1, 2017, to December 31, 2021, used in this study were obtained from five air quality monitoring stations in Daqing City, as shown in Fig. 1: the air quality monitoring stations in Daqing City are Ranghulu District (RHL), Saertu District (SRT), Longfeng District (LF), Hongang District (HG) and Datong District (DT), and the hourly monitoring data of pollutants from the five monitoring stations from the real-time national urban air quality release platform of the China General Environmental Monitoring Station (https://www.mee.gov.cn/). The pollutant concentration data used in this study are hourly monitoring values, and the O_3 concentration data are the eight-hour sliding average of ozone (O3-8h). The data with anomalies and missing data were also excluded and smoothed using monthly averages.

*fangcs@jlu.edu.cn (C.F.)

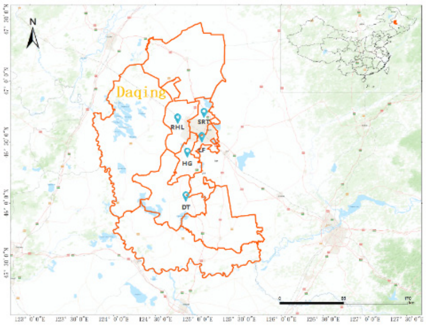

Fig. 1. The research area's location in relation to where the atmospheric monitoring stations are located.

2.2. Research methods

Health Risk Assessment. The health risk evaluation method for site-specific inhalation pathway pollutants (EPA-540-R-070-002) proposed by the US Environmental Protection Agency (EPA) was used to assess the non-carcinogenic and carcinogenic risk values of $PM_{2.5}$ and PM_{10} in air by using their mass concentrations as exposure. In this study, $PM_{2.5}$ and PM_{10} were evaluated for non-carcinogenic risk.

$$ADD = \frac{CA \times IR \times EF \times ED}{BW \times AT} \tag{1}$$

$$HQ_i = \frac{ADD}{RfD} \tag{2}$$

The ADD is the average daily exposure dose of the pollutant; CA is the concentration of the pollutant; IR is the respiratory volume; EF is the exposure frequency; ED is the duration of exposure; AT is the average duration of action d, taking a value of; BW is the average body weight kg; RfD is the average body weight kg. HQ is the hazard quotient of a single pollutant, and when $HQ_i > 1$, it indicates a non-carcinogenic risk.

Principal component analysis (PCA) and Backward trajectory. *Principal component analysis (PCA).* Using principal component analysis to calculate atmospheric pollutants is to treat each atmospheric pollutant as a number of factors to be sought, establish a mathematical model and finally judge the matrix of coefficients of the relationship. So as to obtain the characteristic values of major atmospheric pollutants and their variance contribution [3].

HYSPLIT. We simulated the 72-h backward trajectories at 500 m height in the core city of Daqing City using the HYSPLIT model [4]. In order to facilitate the research of pollutant transport pathways, trajectories were clustered using the stepwise cluster analysis (SCA) algorithm [5]. The equation of SCA is as follows:

$$D = \sqrt{\sum_{j=0}^{t} d_j^2} \tag{3}$$

$$SPVAR = \sum_{i=1}^{x} \sum_{j=0}^{t} d_{ij}^2 \tag{4}$$

$$TSV = \sum SPVAR \tag{5}$$

D is the distance between any two trajectories; *j* is the number of the route point; *t* is the airflow movement time; *i* is the serial number of the backward trajectory; x is the number of trajectories in the cluster; d_j is the distance between the *j* route point of two trajectories; d_{ij} denotes the *j* route point in the *i* backward trajectory to the mean *SPVAR* is the spatial variance of each group of trajectories; *TSV* is the sum of the spatial variance of each group of trajectories. *SPVAR* is the spatial variance of each group of trajectories. [6].

Potential source contribution function (PSCF) analysis. The *PSCF* potential source contribution analysis method was used to identify the pollution source areas. A weighting factor W_{ij} is added to increase the accuracy of $PSCF_{ij}$, and the method is called the weight potential source contribution function WPSCF [7]. Grid-based segmentation first, setting the grid (i, j) resolution to 1° × 1°, and the following equation for the PSCF [8,9].

$$PSCF_{ij} = m_{ij} \times n_{ij} \tag{6}$$

$$W_{ij} = \begin{cases} 1.0, & n_{ij} > 80 \\ 0.7, & 80 \geq n_{ij} > 20 \\ 0.42, & 20 \geq n_{ij} > 10 \\ 0.05, & 10 \geq n_{ij} \end{cases} \tag{7}$$

Multiply $PSCF_{ij}$ with W_{ij} to get the weighted post-WPSCF value of the grid level. The larger the deal, the greater the influence of the grid on the pollutant concentration at the receiving point [10].

3. Results and Discussion

3.1. Analysis of the spatial and temporal distribution characteristics of atmospheric pollutants

Differences in the spatial distribution of pollutant concentrations. The spatial distribution characteristics of the mass concentrations of six air pollutants in Daqing City from 2017 to 2021 were shown in this paper using kriging interpolation. The results are shown in Fig.2. With the development of time, the air pollutants generally show a decreasing trend**.** The concentrations showed a decreasing trend with time. There may be several causes for this pattern in these contaminants' temporal and geographical variations, including firstly, the dominant wind direction in the city of Daqing is northwest, so the northwest direction is the upwind direction, and contaminants from this direction will be blown in the downward direction, causing the accumulation of pollutant concentrations in the southeast order, resulting in a generally greater concentration of pollutants in the northeast direction than in the southwest direction. Secondly, Daqing is a city of oil resources. It has abundant natural gas resources, so there are more gas vehicles on the road, which makes the particulate pollution from traffic within the central city much lower [11].

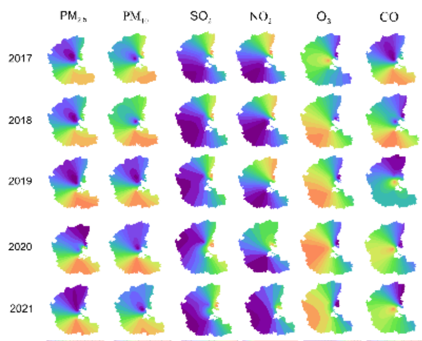

Fig. 2. Six contaminants' spatial distribution of yearly average concentrations from 2017 to 2021.

 https://doi.org/10.1051/e3sconf/202339301022

Monthly variation of pollutant concentrations. Fig. 3 displays the changes in pollutant monthly average concentrations between 2017 and 2021. In terms of monthly medium concentration changes, the monthly variation pattern of O_3 is different, with O_3 concentrations in a gradual increase in the first half of the year and a steady decrease in the second half of the year, with the highest concentration in June and the lowest in December, reflecting the changes in summer concentrations This may be due to the high summer temperatures and stronger solar UV radiation. The concentration of O_3 is also relatively low, and the rise in NO_2 emissions from heating and transportation in winter, as well as the regular occurrence of inversions, causes the NO_2 concentration to be greater in winter.

The remaining contaminants are most prevalent from January through April. The high concentrations of particulate matter, SO_2, and other contaminants in January-March are mainly caused by coal-fired heating, vehicle emissions, and meteorological factors [12].

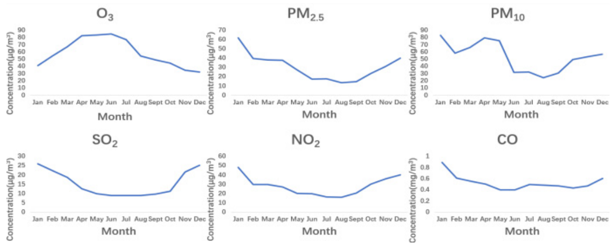

Fig. 3. Six contaminants' monthly concentrations in Daqing City, 2017–2021.

3.2. Health risk assessment analysis

$PM_{2.5}$ and PM_{10} non-carcinogenic risk hazard quotients (HQ) are shown in Fig. 4, with HQ values of 0.326~1.645 for $PM_{2.5}$; 0.576~1.966 for PM_{10}, the highest in winter, followed by spring, and lower in summer and autumn, with some months exceeding the EPA's safety range of less than 1, indicating a potential non-carcinogenic risk level for atmospheric particulate matter in Daqing The Health Effects Institute study suggests that each 10 μ g m^{-3} increase in PM_{10} concentration will cause a 0.6 % increase in daily non-accidental mortality (confidence interval [IC] of 95 %). This effect estimate is similar to or greater than the results of multi-city studies in the USA and Europe [13].

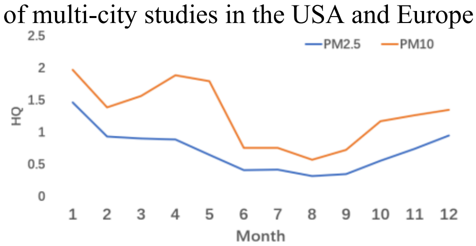

Fig. 4. Trends in HQ values of $PM_{2.5}$ and PM_{10}.

3.3. Principal component analysis of influencing factors

The principal component analysis of the key air pollutants and meteorological circumstances was carried out using SPSS software to identify the main influencing elements of $PM_{2.5}$ engagement. The influencing factors are temperature, air pressure, wind speed, PM_{10}, SO_2, CO, O_3, and NO_2. Since KMO=0.614>0.5 and Bartlett's test approximate chi-square value is 3327.497, corresponding to a probability value of P<0.01, the conditions of principal component analysis are met [14].

The total variance table of the original variables is shown in Table 1.

Table 1. The total variance of the original variables

	Initial Eigenvalue			Extraction of the sum of squares of loads			Sum of squared rotating loads		
Ingredients	Total	Percentage of variance	Cumulative %	Total	Percentage of variance	Cumulative %	Total	Percentage of variance	Cumulative %
1	2.317	28.964	28.964	2.317	28.964	28.964	1.937	24.215	24.215
2	1.493	18.664	47.628	1.493	18.664	47.628	1.634	20.423	44.638
3	1.035	12.939	60.567	1.035	12.939	60.567	1.274	15.929	60.567
4	0.945	11.808	72.375						
5	0.825	10.308	82.683						

The first three components, which have eigenvalues more prominent than 1, and the cumulative contribution rate, which reaches 60.567 %, may individually convey 60.567 % of the properties of the original data, as can be seen from the table above. The first three principal components can be used to represent all variables, which avoids the influence of correlation among independent variables and reduces the dimensionality of the original data, which is beneficial to the study of the original data.

Table 2. The rotated component matrix of principal component analysis

	Ingredients		
	1	2	3
Zscore(T)	-0.054	0.408	-0.656
Zscore(P)	0.089	-0.474	0.099
Zscore(WS)	-0.067	0.651	0.192
Zscore(PM_{10})	0.771	0.241	0.200
Zscore(SO_2)	0.167	0.104	0.823
Zscore(NO_2)	0.706	-0.419	0.191
Zscore(O_3)	0.081	0.747	-0.204
Zscore(CO)	0.892	-0.127	-0.036

Table 2 show that the rotation method is the maximum variance method. The factor loading matrix before and after rotation, it can be seen that the rotated data are more polarized towards 0 and 1, and the relationship between the common factors and the original variables is more straightforward, so the rotated matrix is interpreted as follows.

The first principal component, F1: is closely related to NO_2, CO, and PM_{10}.

The second principal component, F2: is closely related to wind speed and O_3.

The third principal component, F3: is closely related to SO_2 and temperature.

Using SPSS, the main components F1, F2, and F3 and multiple linear regression models of $PM_{2.5}$ concentration were performed. The coefficients of each central element in the model are shown the Sig. values were all less than 0.01, so the regression equation was highly significant.

Bringing the principal component expression obtained in the previous section into the above equation yields:

$C=0.004C1+0.009C2+0.007C3+0.313C4+0.066C5+0.254C6+0.072C7+0.343C8-93.135$

The average temperature, barometric pressure, wind speed, PM_{10}, SO_2, NO_2, O_3, and CO statistics are given in the range C1–C8, where C is the concentration of $PM_{2.5}$.

The model incorporates weather data, air pollution levels, and other variables. It then uses principal component analysis to identify the variables affecting the concentration of $PM_{2.5}$. The findings indicate that the most important variables influencing $PM_{2.5}$ concentration levels are CO, NO_2, and PM_{10}. Therefore, reducing the pollution gases should be the central focus of efforts to reduce $PM_{2.5}$ concentration.

3.4. Cluster analysis

Backward trajectory clustering analysis. The SET monitoring stations in the center of the central city were simulated using the HYSPLIT model to simulate the 72-hour backward trajectories of atmospheric particulate matter for 24 hours per day for the entire year 2021 to cluster them according to differences between trajectories and to analyze the transport paths of particulate matter in different regions [15].

Analysis demonstrates that the spring, fall, and winter seasons have the largest concentrations of northwest-pointing trajectories. Each trajectory's mass concentration of particle matter is attributed to it. The pollution situation is more difficult in spring and winter than in summer and fall. $PM_{2.5}$ mass concentration is 25.31~32.80 μg m^{-3} in the spring. The pollutant mass concentration of PM_{10} is 38.49~124.32 μg m^{-3}, in which the number of trajectories of cluster 4 has the highest proportion and is the main way of airborne particulate pollution transmission in spring; the pollution mass concentration of $PM_{2.5}$ in winter is 24.16~55.46 μg m^{-3}, and the pollutant mass concentration of PM_{10} is 44.28~112.14 μg m^{-3}, of which the trajectory of cluster 1 has the highest proportion of the number of trajectories, which is the main pathway of airborne particulate pollution transmission in winter. The pollution of trajectories in summer and autumn is generally reasonable.

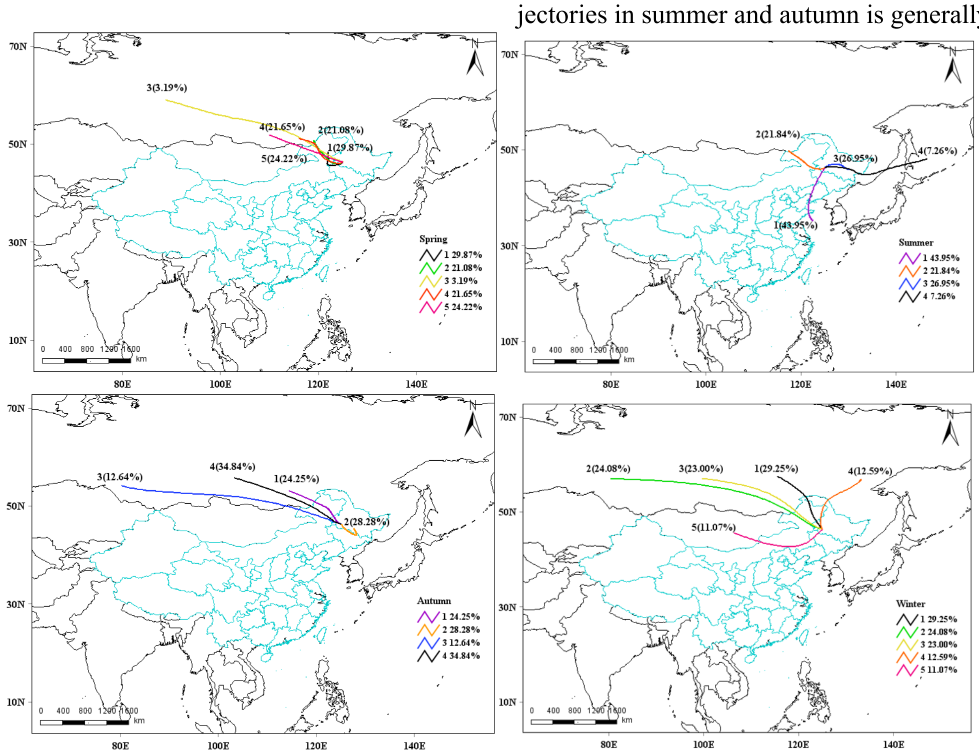

Fig. 5. In 2021, Daqing City's backward trajectory distribution was clustered by season.

Potential source area analysis (PSCF). The backward trajectory analysis can only determine the transport path of pollutants and cannot determine the location and extent of pollution sources. Therefore, the likely source regions of particulate matter are examined and discussed better to assess the atmospheric particulate matter pollution in Daqing city. For $PM_{2.5}$ and PM_{10}, the PSCF establishes concentration thresholds of 150 and 75 μg m^{-3}, respectively. Since the concentration of PM_{10} is generally low in the autumn and summer seasons and there is no polluted airflow after screening by the threshold of 150 μg m^{-3}, the pollution threshold of PM_{10} is defined as 70 μg m^{-3} [16]. The distribution of WPSCF values for $PM_{2.5}$ and PM_{10} in Daqing city by season is depicted in Figure 6,7. Overall, North China, Mongolia, Jilin, Liaoning, and Anhui Provinces make up the majority of the possible sources of pollutants in Daqing City.

The areas with high WPSCF values of PM_{10} in winter and spring are significantly reduced compared with $PM_{2.5}$ and are concentrated in Liaoning Province, Anhui Province, Mongolia, and North China. In addition, there are also small distributions in the territory of Russia and other places, which shows that a lot of $PM_{2.5}$ is released from winter heating; PM_{10} in autumn and summer has a larger WPSCF value in Inner Mongolia, Liaoning Province, Mongolia, North China, and Russia after the pollution threshold adjustment.

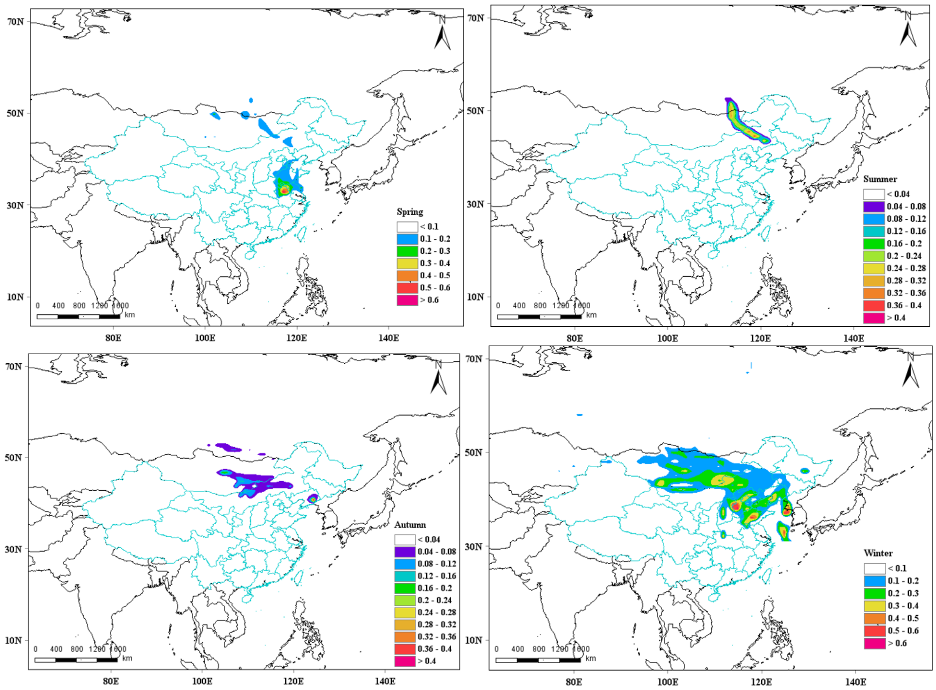

Fig.6. Characteristics of the seasonal distribution of $PM_{2.5}$ WPSCF values in Daqing City in 2021.

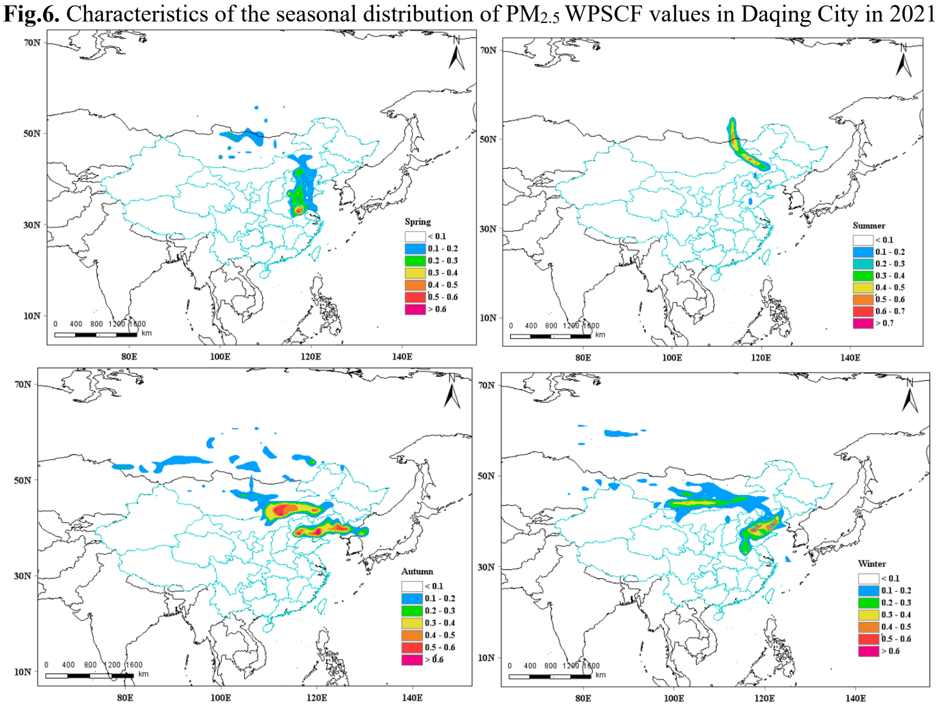

Fig.7. Characteristics of the seasonal distribution of PM_{10} WPSCF values in Daqing City in 2021.

4.CONCLUSIONS

(1) The research region was examined using the Kriging interpolation technique. The investigation demonstrates that SO_2 and NO_2, which are affected by plant cover and chemical reaction processes, are more significant in the central urban area and lower in the suburban region. The opposite is true for O_3. The other pollutants are higher in the south and lower in the north because the dominant wind direction in Daqing is northwest, and the concentration of pollutants will accumulate downwind.

(2) The monthly changes of ozone are analyzed in terms of monthly changes: The concentration of O_3 continuously drops in the second half of the year and gradually rises in the first, which may be related to the greater UV radiation in the summer, which is beneficial for the production of O_3. Since NO_2 and O_3 can be transformed into each other, the changes of NO_2 and O_3 have roughly opposite trends.

(3) The hazard quotient (HQ) for atmospheric particulate matter, which is slightly above the safe range set by the EPA, is higher in winter and spring, and the potential

non-carcinogenic risk is higher and should be taken seriously.

(4) According to the $PM_{2.5}$ principal component analysis, three components have eigenvalues larger than 1, and their combined contribution is 60.567 %. Therefore, it is still required to manage the polluting gas to control the particulate matter pollution since regression study has shown that CO, NO_2, and PM_{10} are the most important variables impacting the concentration value of $PM_{2.5}$.

(5) The HYSPLIT model's backward trajectory simulation analysis of the research region reveals that the northwest direction primarily affects spring, fall, and winter whereas the southeast direction primarily affects summer. It can be seen that the pollution problem is worse in the spring and winter, and that the main routes for regional pollution transmission in Daqing City are the northwest trajectory through Russia, Mongolia, and Inner Mongolia, and the southwest trajectory through North China and Jilin Province.

(6) The potential particle source areas were investigated using the PSCF model. A broad range of sources may contribute to particulate matter throughout the winter and spring. The possible source region of particulate matter in the summer and fall has low WPSCF values. After adjusting the threshold value of PM_{10}, it can be found that the possible source area in summer is striped and covers a small space, mainly in Inner Mongolia, Mongolia, and Russia. The potential source area in autumn covers a larger area, mainly in Inner Mongolia, Mongolia, and North China.

References

1. Chen W W, Zhang S C, Tong D Q, et al. (2018) Regional Characteristics and Causes of Haze Events in Northeast China [J]. Chinese Geographical Science, 28 (5): 836-850. https://doi.org/10.1007/s11769-018-0965-3.
2. Pala K, Aykac N, Yasin Y. (2021) Premature deaths attributable to long-term exposure to $PM_{2.5}$ in Turkey [J]. Environmental Science and Pollution Research International, 37: 51940-51947. https://doi.org/10.1007/s11356-021-13923-5.
3. Jiang X H, Xue H, Zhang C H, et al. (2016) Comparative analysis of air quality between Beijing and Hohhot [J]. Safety and Environmental Engineering, 23(1): 75-79. https://doi.org/10.12153/j.issn.1674-991X.20210214.
4. Jr I H B, Meeker G O. (2013) A factor analysis model of largescale pollution [J]. Atmospheric Environment, 1(2): 147-157. https://doi.org/10.1016/0004-6981(67)90042-X.
5. Urlea A D, Barbu N, Andrei S, et al. (2021) Simulation of Vesuvius volcanic ash hazards within Romanian airspace using the Hybrid Single Particle Lagrangian Integrated Trajectory Volcanic Ash numerical model [J]. Meteorological Applications, 28. https://doi.org/10.1002/met.2001.
6. Fang C, Gao J, Wang D, et al. (2020) Optimization of stepwise clustering algorithm in backward trajectory analysis [J]. Neural Computing and Applications, 32: 109-115. https://doi.org/10.1002/met.2001.
7. Dimitriou K, Kassomenos P. (2016) Combining AOT, Angstrom Exponent and $PM_{2.5}$ concentration data, with PSCF model, to distinguish fine and coarse aerosol intrusions in Southern France [J]. Atmospheric Environment, 172: 74-82. https://doi.org/10.1016/J.ATMOSRES.2016.01.002.
8. Sun J, Huang L, Liao H, et al. (2017) Impacts of Regional Transport on Particulate Matter Pollution in China: a Review of Methods and Results [J]. Current Pollution Reports, 3: 182-191. https://doi.org/10.1007/s40726-017-0065-5.
9. Dimitriou K, Kassomenos P. (2014) Indicators reflecting local and transboundary sources of $PM_{2.5}$ and PM COARSE in Rome-Impacts in air quality [J]. Atmospheric Environment, 96: 154-162. https://doi.org/10.1016/j.atmosenv.2014.07.029.
10. Hong Q Q, Liu C, Hu Q H, et al. (2019) Evolution of the vertical structure of air pollutants during winter heavy pollution episodes: The role of regional transport and potential sources [J]. Atmosphere research, 228: 206-222. https://doi.org/10.1016/j.atmosres.2019.05.016.
11. Lou C R, Liu H Y, Li Y F, et al. (2016) Socioeconomic Drivers of $PM_{2.5}$ in the Accumulation Phase of Air Pollution Episodes in the Yangtze River Delta [J]. Environment research public health, 13: 928. https://doi.org/10.1016/j.atmosres.2019.05.016.
12. Yao Y, He C, Li S, et al. (2019) Properties of particulate matter and gaseous pollutants in Shandong, China: daily fluctuation, influencing factors, and spatiotemporal distribution [J]. Science of The Total Environment, 660: 384-394. https://doi.org/10.1016/j.scitotenv.2019.01.026.
13. Analitis, A.（2006） Short-term effects of ambient particles on cardiovascular and respiratory mortality. Epidemiology, 17(2): 230-3. https://doi.org/10.1097/01.ede.0000199439.57655.6b.
14. Otmani A, Benchrif A, Tahri M, et al. (2020) Impact of COVID-19 lockdown on PM_{10}, SO_2 and NO_2 concentrations in Sale City (Morocco) [J]. Science of The Total Environment, 735: 139541. https://doi.org/10.1016/j.scitotenv.2020.139541. https://doi.org/10.1175/BAMS-D-14-00110.1.
15. Stein A F, Draxler R R, Rolph G D, et al. (2015) NOAA's HYSPLIT Atmospheric Transport and Dispersion Modeling System [J]. American Meteorological Society, 96: 2059-2077. https://doi.org/10.1175/BAMS-D-14-00110.1.
16. Zhou S, Liu N, Liu C S. (2017) Identification for potential sources for haze events in Shanghai from 2013 to 2015 [J]. Acta Scientiae Circumstantiae, 37(5): 1835-1842. http://dx.doi.org/10.13671/j.hjkxxb.2016.0356.